

Electron spin resonance studies of silver complexes of octaethylporphyrin cocrystallized with fullerenes: observation of triplet spin states due to magnetic dipolar interactions

This article has been downloaded from IOPscience. Please scroll down to see the full text article.

2004 J. Phys.: Condens. Matter 16 8753

(<http://iopscience.iop.org/0953-8984/16/47/025>)

View [the table of contents for this issue](#), or go to the [journal homepage](#) for more

Download details:

IP Address: 129.252.86.83

The article was downloaded on 27/05/2010 at 19:13

Please note that [terms and conditions apply](#).

# Electron spin resonance studies of silver complexes of octaethylporphyrin cocrystallized with fullerenes: observation of triplet spin states due to magnetic dipolar interactions

K Marumoto<sup>1</sup>, H Takahashi<sup>1</sup>, H Tanaka<sup>1</sup>, S Kuroda<sup>1</sup>, T Ishii<sup>2</sup>,  
R Kanehama<sup>3</sup>, N Aizawa<sup>3</sup> and M Yamashita<sup>3,4</sup>

<sup>1</sup> Department of Applied Physics, Nagoya University, Chikusa-ku, Nagoya 464-8603, Japan

<sup>2</sup> Department of Advanced Materials Science, Kagawa University, Hayashi-cho 2217-20, Takamatsu 761-0396, Japan

<sup>3</sup> Department of Chemistry, Tokyo Metropolitan University and CREST (JST), 1-1 Minamioshima, Hachioji 192-0397, Japan

Received 18 June 2004, in final form 3 September 2004

Published 12 November 2004

Online at [stacks.iop.org/JPhysCM/16/8753](http://stacks.iop.org/JPhysCM/16/8753)

doi:10.1088/0953-8984/16/47/025

## Abstract

Electron spin resonance (ESR) studies have been performed on newly synthesized Ag<sup>II</sup> complexes of octaethylporphyrin (oep) cocrystallized with fullerenes (C<sub>60</sub> and C<sub>70</sub>) using single crystals and polycrystals between 4 and 300 K. We have observed the fine structure in the ESR spectra of Ag<sup>II</sup>(oep)C<sub>60</sub>; the fine structure is ascribed to the triplet spin states due to magnetic dipolar interactions between  $S = 1/2$  spins of Ag<sup>II</sup> ions in adjacent oep molecules. The analysis of the angular dependence of the  $g$  value and fine-structure splitting width for Ag<sup>II</sup>(oep)C<sub>60</sub> single crystals determines the angle between the Ag–Ag direction and the normal of the Ag–oep plane as 37°. The results of Ag<sup>II</sup>(oep)C<sub>70</sub> are similar to those of Ag<sup>II</sup>(oep)C<sub>60</sub>. The spin susceptibility of all complexes almost obeys the Curie law, indicating the exchange interactions between the spins of Ag ions are negligible in the temperature region measured.

## 1. Introduction

The unique three-dimensional shapes of the fullerenes coupled with their distinct physical properties such as superconductivity, ferromagnetism, etc make them attractive candidates for the construction of large, supramolecular aggregates [1–3]. The ball-shaped fullerenes such as C<sub>60</sub> and C<sub>70</sub> have been reported to be not appropriate to cocrystallize with planar

<sup>4</sup> Present address: Department of Chemistry, Tohoku University and CREST (JST), Aoba-ku, Sendai 980-8578, Japan.

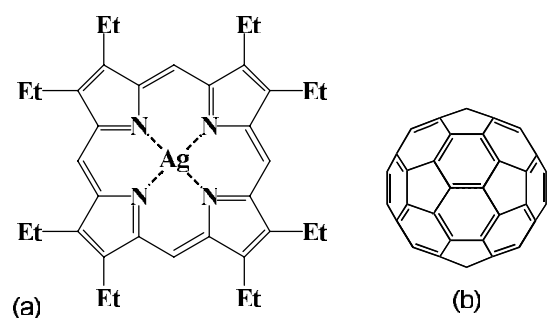


**Figure 1.** Chemical structures of (a) silver (Ag)-octaethylporphyrin (oep) complex and (b) fullerene (C<sub>60</sub>).

molecules, and curving of the planar molecule is required to be fitted to the ball-shaped fullerenes [4, 5]. Recently, transition metal complexes of porphyrin derivative, such as metal octaethylporphyrin (oep) (see figure 1(a)), cocrystallized with fullerenes, have been reported to form solids with remarkably close contact between the curved  $\pi$ -surface of fullerenes and the planar  $\pi$ -surface of the porphyrin, without need for matching a convex with a concave surface [6–14]. These complexes construct a new type of  $\pi$ -d electron system, that is, magnetic d electrons due to the metal complex of the porphyrin and conductive  $\pi$  electrons due to fullerenes, which have been studied by means of x-ray structural analyses, nuclear magnetic resonance, electron spin resonance (ESR), etc. They are considered as possible precursors for three-dimensional molecular magnets and are also expected to create other new functions [15]. In order to produce the magnetism in these cocrystallites, the magnetic interactions such as exchange and dipolar interactions between the constituent molecules are important. For d-d type exchange interactions via the C<sub>60</sub> molecule, the antiferromagnetic super-exchange interaction between Co<sup>II</sup> ions via C<sub>60</sub> in Co<sup>II</sup>(tbp)C<sub>60</sub> is confirmed by the ESR studies [13], where tbp is 5, 10, 15, 20-tetrakis[3,5-(di-*tert*-butyl)-phenyl]porphyrin. For d-d magnetic dipolar interactions, the ESR spectra of the powder compound (CuPz)<sub>2</sub>C<sub>60</sub> show a binuclear triplet spin state ( $S = 1$ ) that is associated with the ‘back-to-back’ Cu(Pz) pairs, where Pz is octakis(dimethylamino)porphyrazinato [8]. Thus, the ESR method is a powerful technique to study spin states in these complexes, as also demonstrated in the studies of the composites of fullerenes and conducting polymers [16, 17]. This method will also obtain the knowledge of the magnetic properties of other  $\pi$ -d electron systems. However, except for Co<sup>II</sup>(tbp)C<sub>60</sub> and (CuPz)<sub>2</sub>C<sub>60</sub>, detailed ESR study using single crystals has not been performed on the metal complexes of porphyrin cocrystallized with fullerenes, and spin states of these complexes have not been investigated in detail so far.

In this paper we report on the ESR studies of newly synthesized metal complexes of oep cocrystallized with fullerenes, that is, Ag<sup>II</sup>(oep)C<sub>60</sub> and Ag<sup>II</sup>(oep)C<sub>70</sub> [10, 18], using single crystals and polycrystals. The paper is organized as follows: after describing the experimental procedure in section 2, we present the temperature and angular dependence of the ESR spectra and the ESR parameters such as the spin susceptibility  $\chi_s$  and the  $g$  value in section 3. First, we present the ESR results of Ag<sup>II</sup>(oep)C<sub>60</sub>. The ESR spectra and temperature dependence of the  $\chi_s$  of Ag<sup>II</sup>(oep)C<sub>60</sub> polycrystals are presented in section 3.1, where the fine structure due to magnetic dipolar interactions between  $S = 1/2$  spins of Ag<sup>II</sup> ions is discussed. The angular dependence of the  $g$  value and fine-structure splitting width of Ag<sup>II</sup>(oep)C<sub>60</sub> single crystals are presented in section 3.2, where the results are analysed by a spin-pair model. Second, we comment on the ESR results of Ag<sup>II</sup>(oep)C<sub>70</sub> and compare the results with that of Ag<sup>II</sup>(oep)C<sub>60</sub> in section 3.3. We summarize our results in section 4.

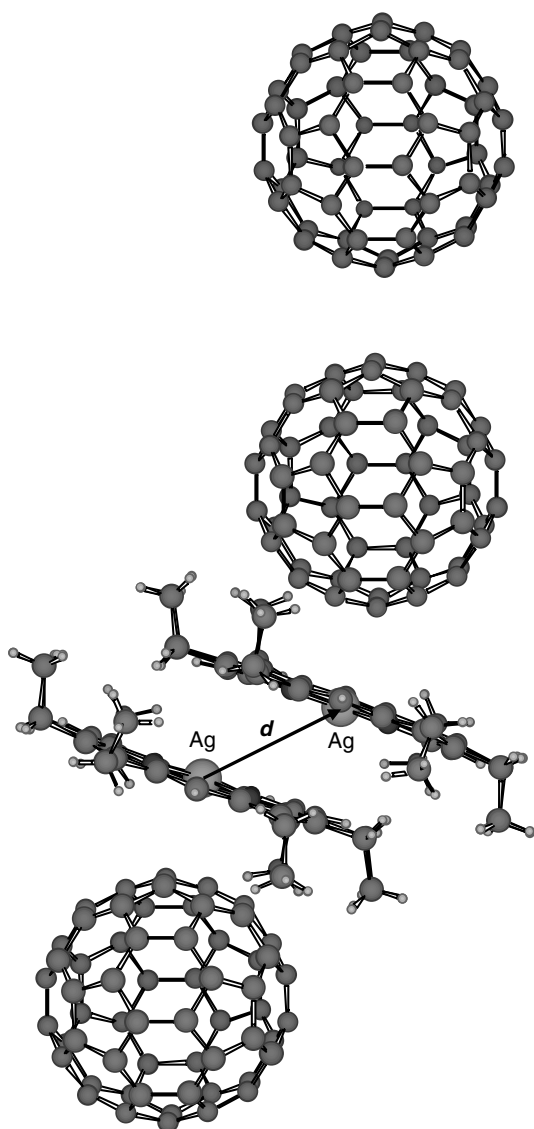


**Figure 2.** A view of the molecular packing in  $\text{Ag}^{\text{II}}(\text{oep})\text{C}_{60}$  determined by the x-ray analyses [10]. Two Ag ions in the two adjacent oep molecules are marked.  $d$  denotes the vector of the fine-structure interaction. Two fullerenes are symmetrically positioned between two  $\text{Ag}^{\text{II}}(\text{oep})$  units, and the fullerene is too far from the atoms of the  $\text{Ag}^{\text{II}}(\text{oep})$  for any covalent bonding between them. The details are described in [10].

## 2. Experimental details

The chemical structures of Ag–oep and  $\text{C}_{60}$  are shown in figures 1(a) and (b), respectively. The single-crystalline and polycrystalline samples of  $\text{Ag}^{\text{II}}(\text{oep})\text{C}_{60}$  and  $\text{Ag}^{\text{II}}(\text{oep})\text{C}_{70}$  have been synthesized by diffusion and evaporation of a mixture of a solution of the fullerene ( $\text{C}_{60}$  and  $\text{C}_{70}$ ) in benzene and a solution of the  $\text{Ag}^{\text{II}}(\text{oep})$  in chloroform as described elsewhere [10, 18]. A view of the molecular packing in  $\text{Ag}^{\text{II}}(\text{oep})\text{C}_{60}$  is shown in figure 2; the packing has been determined by x-ray analyses [10]. The oep molecule takes two different configurations

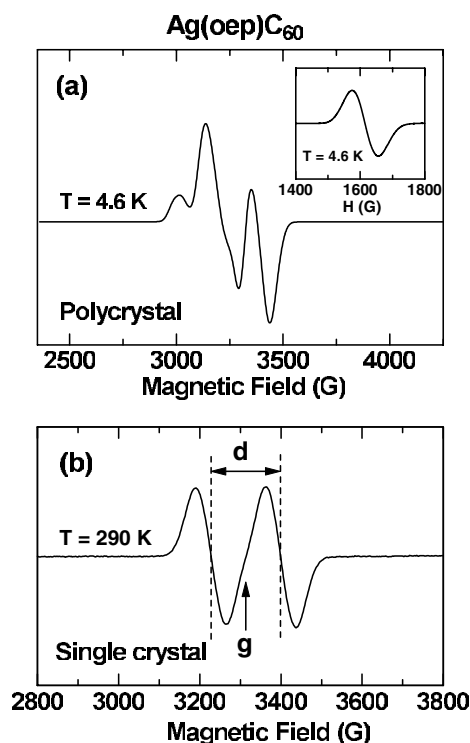


**Figure 3.** (a) The ESR spectrum of  $\text{Ag}^{\text{II}}(\text{oep})\text{C}_{60}$  polycrystalline samples at 4.6 K. Inset: ESR spectrum of  $\text{Ag}^{\text{II}}(\text{oep})\text{C}_{60}$  polycrystalline samples at half field of  $\sim 1600$  G at 4.6 K. (b) A typical ESR spectrum of an  $\text{Ag}^{\text{II}}(\text{oep})\text{C}_{60}$  single-crystalline sample at 290 K. The definition of the  $g$  value and the fine-structure splitting width  $d$  is presented, where the field corresponding to the  $g$  value is determined as a mid-point of the fine-structure splitting.

in these cocrystallites: the *anti*-formed oep in  $\text{Ag}^{\text{II}}(\text{oep})\text{C}_{60}$  and the *syn*-formed oep in  $\text{Ag}^{\text{II}}(\text{oep})\text{C}_{70}$  [10, 12, 18]<sup>5</sup>.

The  $\text{Ag}(\text{II})$  state in  $\text{Ag}^{\text{II}}(\text{oep})\text{C}_{60}$  has been described in the previous papers [10, 12], where the reduction states of oep and  $\text{C}_{60}$  are  $-2$  and zero, respectively, and there is no charge transfer to  $\text{C}_{60}$ . The ESR study on the Ag–porphyrin complex has also directly demonstrated the  $\text{Ag}(\text{II})$  state [20]. As will be discussed below, the  $\text{Ag}(\text{II})$  states in  $\text{Ag}^{\text{II}}(\text{oep})\text{C}_{60}$  and  $\text{Ag}^{\text{II}}(\text{oep})\text{C}_{70}$  are also confirmed by the present ESR results, that is, an anisotropy of the  $g$  value in the ESR spectra of  $\text{Ag}^{\text{II}}(\text{oep})\text{C}_{60}$  single crystal and similarities of the powder pattern of the ESR spectra between  $\text{Ag}^{\text{II}}(\text{oep})\text{C}_{60}$  and  $\text{Ag}^{\text{II}}(\text{oep})\text{C}_{70}$ .

ESR measurements were performed by using a Bruker EMX *X*-band spectrometer equipped with an Oxford ESR-900 gas-flow cryostat. Sample temperature was controlled by an Oxford ITC 601. The spin susceptibility  $\chi_s$  was obtained by integrating the first-derivative ESR spectrum twice. The absolute magnitude of the  $\chi_s$  and  $g$  values was calibrated using  $\text{CuSO}_4 \cdot 5\text{H}_2\text{O}$  and diphenylpicrylhydrazyl (DPPH) as the standard, respectively. The single-crystalline samples were mounted on a Teflon sample holder using normal silicon grease.

<sup>5</sup> The term '*anti*' in this paper denotes the *anti*-symmetry of the terminal eight ethyl groups on the porphyrin plane according to the *E, Z*-nomenclature. This is a different meaning from a so-called *anti*-compound mentioned by Balch and Olmstead [19].

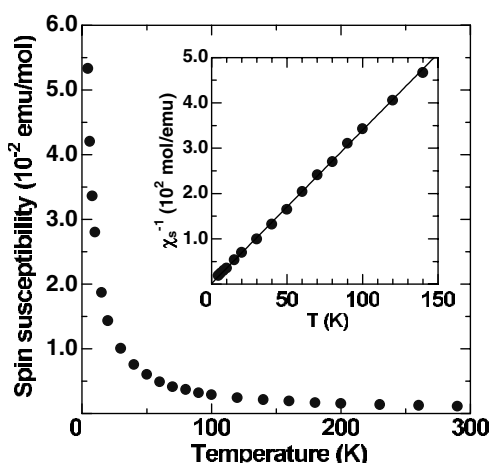


**Figure 4.** Temperature dependence of the spin susceptibility  $\chi_s$  of  $\text{Ag}^{\text{II}}(\text{oep})\text{C}_{60}$  polycrystalline samples. Inset: temperature dependence of the inverted  $\chi_s$  of  $\text{Ag}^{\text{II}}(\text{oep})\text{C}_{60}$  polycrystalline samples. The solid line denotes the fitting by the Curie–Weiss law.

### 3. Results and discussion

#### 3.1. $\text{Ag}^{\text{I}}(\text{oep})\text{C}_{60}$ polycrystal

In this subsection, we present the ESR spectra and the temperature dependence of spin susceptibility  $\chi_s$  of  $\text{Ag}^{\text{II}}(\text{oep})\text{C}_{60}$  polycrystalline samples, which show the triplet spin states due to magnetic dipolar interactions without exchange interactions between the spin species.

Figure 3(a) shows the ESR spectrum of  $\text{Ag}^{\text{II}}(\text{oep})\text{C}_{60}$  polycrystalline samples. The inset of figure 3(a) shows the ESR spectrum at half field that is related to the forbidden transition ( $\Delta M = 2$ ). The line shapes of these spectra are confirmed to be almost independent of the temperature between 4 and 300 K. The structure in the ESR spectra is ascribed to the fine structure of the triplet spin state ( $S = 1$ ) due to magnetic dipolar coupling of  $\text{Ag}^{\text{II}}$  spins ( $S = 1/2$ ) in the adjacent oep molecules, because the hyperfine-coupling constant of Ag nucleus ( $I = 1/2$ ) in the Ag–porphyrin complex is reported as  $\sim 30\text{--}70$  G [20], that cannot explain the observed ESR structure. The triplet spin state is directly confirmed by the forbidden transition at half field (see the inset of figure 3(a)). Further support is obtained by the study using single crystals, as will be discussed in section 3.2. We have also performed the ESR measurements using completely powdered samples; the obtained ESR spectra are confirmed to be almost the same as those of polycrystalline samples.

Figure 4 and its inset show the temperature dependence of the spin susceptibility  $\chi_s$  and inverted  $\chi_s$  of  $\text{Ag}^{\text{II}}(\text{oep})\text{C}_{60}$  polycrystalline samples. The solid line in the inset shows a least squares fit of the data to the Curie–Weiss law [ $\chi = C/(T - \theta)$ ]. The data almost obey the Curie law; the antiferromagnetic Weiss temperature is obtained as  $\sim -0.7$  K. This feature indicates that the spin species have almost no exchange interaction with another spin species in the temperature region between 4 and 300 K. The Curie-spin concentration is obtained as  $\approx 100\%$ . The intensity of the ESR signal of  $g \sim 4$  shown in the inset of figure 3(a) is also confirmed to obey the Curie law. Here, we estimate the magnitude of the fine-structure constant  $D$ . Let the spin susceptibility of the  $g \sim 4$  signal be  $\chi_s^{g^4}$ , that is obtained by integrating the signal of the  $g \sim 4$  line only, then we may approximate the forbidden-transition probability  $(D/g\mu_B H)^2$  at the ESR intensity ratio of  $\chi_s^{g^4}/\chi_s$ , that is,  $\chi_s^{g^4}/\chi_s \sim (D/g\mu_B H)^2$  [21, 22]. By this relation, the value of  $D$  is estimated as of the order of  $10^{-2} \text{ cm}^{-1}$ .

In the study of  $\text{Co}^{\text{II}}(\text{tbp})\text{C}_{60}$ , the antiferromagnetic super-exchange interaction between  $\text{Co}^{\text{II}}$  ions via the  $\text{C}_{60}$  molecule is confirmed along the  $z$ -axis (parallel to the normal of the  $\text{tbp}$  plane) with the finite Weiss temperature of 4.9 K, although the  $\text{Co}^{\text{II}}\text{--Co}^{\text{II}}$  distance itself is rather large: 12.0635(8) Å at room temperature [13]. The super-exchange interaction is ascribed to the overlapping of the wavefunction between the  $d_{z^2}$  electron orbital of the low-spin  $\text{Co}^{\text{II}}$  ions ( $S = 1/2$ ) and the  $\pi$  electron orbital of  $\text{C}_{60}$ , because of a quite short distance between a  $\text{Co}^{\text{II}}$  ion and a carbon atom on  $\text{C}_{60}$  (2.61 Å at 293 K) [11]. Such close contact makes possible covalent bonding between the above wavefunctions. On the other hand, in the present  $\text{Ag}^{\text{II}}(\text{oep})\text{C}_{60}$ , the wavefunction of the  $d_{x^2-y^2}$  hole orbital of an  $\text{Ag}^{\text{II}}$  ion extends to the  $\text{oep}$  plane, not to the  $\text{C}_{60}$  molecule, and hence, the super-exchange interaction between  $\text{Ag}^{\text{II}}$  ions via the  $\text{C}_{60}$  molecule is considered negligibly small. Thus, for the purposes of introducing the exchange interaction between metal ions via the  $\text{C}_{60}$  molecule, we should use metal ions having a  $d_{z^2}$  or  $d_{zx,yz}$  orbital such as the low-spin  $\text{Co}^{\text{II}}$  ions in these cocrystallites.

### 3.2. $\text{Ag}^{\text{II}}(\text{oep})\text{C}_{60}$ single crystal

In this subsection, we present the angular dependences of the  $g$  value and fine-structure splitting width of the ESR spectra of the  $\text{Ag}^{\text{II}}(\text{oep})\text{C}_{60}$  single crystal, which are analysed by using a spin-pair model.

Figure 3(b) shows a typical ESR spectrum of the  $\text{Ag}^{\text{II}}(\text{oep})\text{C}_{60}$  single-crystalline sample at 290 K. Two split ESR signals are clearly observed owing to the fine-structure splitting. We define the  $g$  value and the fine-structure splitting width  $d$  as shown in figure 3(b), where the field corresponding to the  $g$  value is determined as a mid-point of the fine-structure splitting. The hyperfine splitting due to  $^{107,109}\text{Ag}$  nuclear spin and the super-hyperfine splittings due to four nitrogen  $^{14}\text{N}$  nuclear spins ( $I = 1$ ) are unresolved and probably contribute the linewidth of each ESR signal with the peak-to-peak linewidth  $\Delta H_{\text{pp}}$  of 75 G, because the maximum shift of the resonance field due to the Ag and N nuclear spins in the Ag–porphyrin complex is reported as  $\sim 100$  G [20]. These structures due to the hyper- and super-hyperfine splittings are masked owing to the broadening of the linewidth due to the dipolar magnetic interactions from another  $\text{oep}$  pair, because the dipolar field is estimated as the order of 10 G by considering the dimension of the unit cell [10]. The  $\Delta H_{\text{pp}}$  for the external magnetic field  $H$  parallel to the normal of the  $\text{oep}$  plane is almost the same as that perpendicular to the  $\text{oep}$  plane. This feature is consistent with the reported result that the maximum shift of the resonance field due to the Ag and N nuclei for  $H$  parallel to the normal in the Ag–porphyrin complex is almost the same as that perpendicular to the normal, that is,  $A_{\parallel}^{\text{Ag}}/2 + 4A_{\parallel}^{\text{N}} \approx A_{\perp}^{\text{Ag}}/2 + 4A_{\perp}^{\text{N}}$ , where the hyperfine-coupling constant of Ag for  $H$  parallel to the normal  $A_{\parallel}^{\text{Ag}}$  (72 G) is larger than that perpendicular to the normal  $A_{\perp}^{\text{Ag}}$  (34 G) while the super-hyperfine-coupling constant of N for  $H$  parallel to the normal  $A_{\parallel}^{\text{N}}$  (20 G) is smaller than that perpendicular to the normal  $A_{\perp}^{\text{N}}$  (25 G) [20].

Figures 5(a) and (b) show the angular dependence of the  $g$  value, and figures 5(c) and (d) show the angular dependence of the fine-structure splitting width  $d$  at 290 K. Here, the square plate schematically denotes the Ag– $\text{oep}$  plane in order to present the experimental condition for rotating the sample with respect to the external magnetic field. In figures 5(a) and (c), the external magnetic field is applied in the plane of the Ag– $\text{oep}$  molecule. In figures 5(b) and (d), the external magnetic field is applied in the plane containing the normal of the Ag– $\text{oep}$  molecule. The angular variation of the  $g$  value shows the uniaxial anisotropy; this result is consistent with the fourfold coordination symmetry of the crystal field acting on an  $\text{Ag}^{\text{II}}$  ion by the  $\text{oep}$  molecule (see figure 1(a)). The principal values of  $g$  are determined as  $g_{\perp} = 2.028 \pm 0.002$

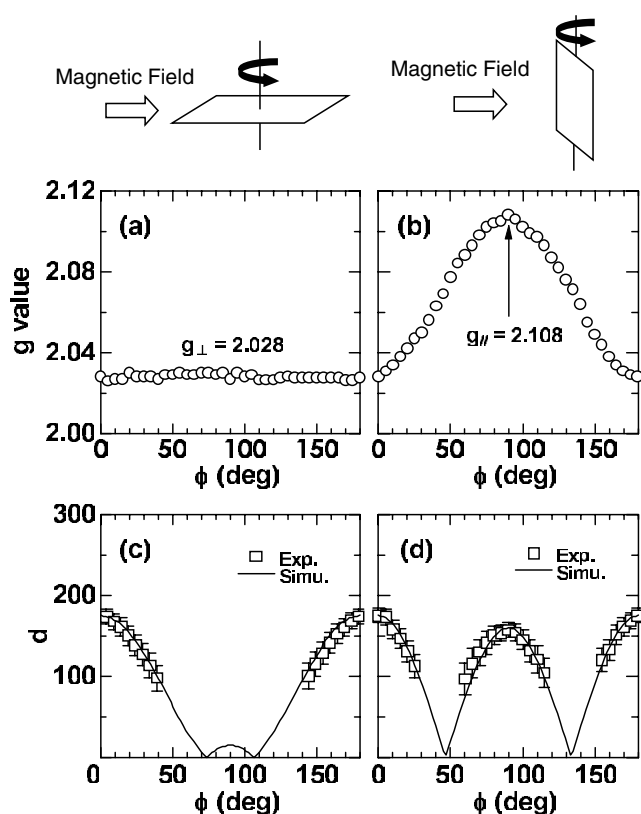


**Figure 5.** Angular dependence of the  $g$  value ((a) and (b)) and the fine-structure splitting width  $d$  ((c) and (d)) of the  $\text{Ag}^{\text{II}}(\text{oep})\text{C}_{60}$  single crystal at 290 K. The abscissa  $\phi$  denotes the rotation angle of the sample. Square plates schematically denote the plane of the Ag–oep molecule. In (a) and (c), the sample is rotated in the plane of the Ag–oep molecule. In (b) and (d), the sample is rotated in the plane containing the normal of the Ag–oep molecule. The solid curves in (c) and (d) show the fitting results of the simulation using a point-dipole model expressed by equations (3) and (4), respectively.

and  $g_{\parallel} = 2.108 \pm 0.002$ . Here,  $g_{\parallel}$  and  $g_{\perp}$  denote the  $g$  value parallel and perpendicular to the normal of the Ag–oep molecule, respectively. Both principal values are larger than the free-electron  $g$  value ( $g_e = 2.0023$ ), which is consistent with the crystal-field calculation with the unpaired electron residing on the  $\text{Ag}(d_{x^2-y^2})$  orbital [21]. Let the spin–orbit coupling constant in the crystal be  $\lambda$  ( $\lambda < 0$  for the  $d^9$  configuration), the energy of the tetragonal crystal-field splitting between  $d_{x^2-y^2}$  and  $d_{zx}$ ,  $d_{yz}$  orbitals be  $\Delta_{\perp}$ , and the energy between  $d_{x^2-y^2}$  and  $d_{xy}$  orbitals be  $\Delta_{\parallel}$  ( $\Delta_{\perp} > \Delta_{\parallel}$ ), then the calculated  $g$  values based on the crystal-field theory are expressed as

$$g_{\perp} = g_e - 2 \frac{\lambda}{\Delta_{\perp}}, \quad g_{\parallel} = g_e - 8 \frac{\lambda}{\Delta_{\parallel}}. \quad (1)$$

These equations clearly explain the observed anisotropy of the  $g$  values. On the other hand, the fine-structure splitting width  $d$  due to magnetic dipole–dipole interactions between  $\text{Ag}^{\text{II}}$  ions disappears at so-called magic angles as shown in figures 5(c) and (d). The absence of the data of  $d < \sim 100$  G is ascribed to unresolved fine structure of the ESR spectra around the magic angles. In the present cocrystallite, the direction of the fine-structure interaction and the principal axes of the  $g$  values are different from each other (see figure 2), where the rotation



plane of the external magnetic field does not include the direction of the dipolar interaction in general. Therefore, the magic angles observed in this experiment deviate from the usual values of  $54^\circ$  and  $126^\circ$ , and appear in both sample-rotation directions (see figures 5(c) and (d)).

We have analysed the above angular dependence of the fine-structure splitting width  $d$  using a spin-pair model for the  $\text{Ag}^{\text{II}}$  ions on adjacent oep molecules. Let the fine-structure constant be  $D$ , the Ag–Ag direction vector of the fine-structure interaction be  $\mathbf{d}$ , and the angle between  $\mathbf{d}$  and the direction of the external magnetic field be  $\Theta$ , then we may write the formula of  $d$  as

$$d = |D (3 (\cos \Theta)^2 - 1)|. \quad (2)$$

Here, the  $E$  term is eliminated, because the contribution from the  $E$  term is found to be considerably small by the analysis with the additional  $E$  term in the present complex. From now on, the oep plane is defined as the  $x'y'$ -plane and the normal of the Ag–oep plane is defined as the  $z'$ -axis. The external magnetic field  $\mathbf{H}$  is applied in the direction of the  $y'$ -axis; that is,  $\mathbf{H} = (0, H, 0)$ . Let the angle between  $\mathbf{d}$  and the  $z$ -axis be  $\theta$ , and the rotation angle of the sample be  $\phi$ , then the vector  $\mathbf{d}$  is expressed as  $\mathbf{d} = (|d| \sin \theta \cos \phi, |d| \sin \theta \sin \phi, |d| \cos \theta)$ . Hence,  $\mathbf{d} \cdot \mathbf{H} \equiv |d||H| \cos \Theta$  is expressed as  $|d||H| \sin \theta \sin \phi$ ; that is,  $\cos \Theta = \sin \theta \sin \phi$ . Therefore, for the case in figure 5(c), that is, the sample is rotated in the  $x'y'$ -plane, we may write the simulation formula of  $d$  as

$$d = |D (3 (\sin \theta \sin \phi)^2 - 1)|, \quad (3)$$

where  $\mathbf{d}$  is in the  $z'x'$ -plane when  $\phi = 0^\circ$ . Similarly, for the case in figure 5(d), that is, the sample is rotated in the  $y'z'$ -plane of the Ag–oep molecule,  $\mathbf{d}$  is expressed as  $\mathbf{d} = (|d| \cos(90^\circ - \theta), |d| \sin(90^\circ - \theta) \sin(-\phi), |d| \sin(90^\circ - \theta) \cos(-\phi))$ , and then we may write the simulation formula of  $d$  as

$$d = |D (3 (\sin(90^\circ - \theta) \sin \phi)^2 - 1)|. \quad (4)$$

Here, when  $\phi = 0^\circ$ ,  $\mathbf{d}$  is in the  $z'x'$ -plane and the oep plane is in the  $x'y'$ -plane. The fitting parameters are  $\theta$  and the fine-structure constant  $D$ . The best-fitting results of the simulation are shown in figures 5(c) and (d) by solid curves. The characteristic angular dependence of the splitting width is well explained by the spin-pair model. The values of the parameters are determined as  $\theta = 37 \pm 1^\circ$  and  $D = 1.6 \times 10^{-2} \text{ cm}^{-1}$ . The result of  $\theta = 37^\circ$  is consistent with x-ray results (see figure 2) [10, 12]. The  $D$  value obtained is of the same order as that estimated by the ESR intensity ratio of  $\chi_s^{g4}/\chi_s$  obtained by the polycrystalline measurement.

In the ESR studies of  $(\text{CuPz})_2\text{C}_{60}$ , the Cu–Cu distance has been estimated by the point-dipole model as  $4.3 \text{ \AA}$ , that approximates the crystal data of  $4.78 \text{ \AA}$  [8]. On the other hand, in the Ag–oep complex, the simple point-dipole model does not give the Ag–Ag distance of  $4.475 \text{ \AA}$  reported by the x-ray analysis [10, 12], because the spatial extent of the Ag  $4d_{x^2-y^2}$  orbital is larger than that of the Cu  $3d_{x^2-y^2}$  orbital and hence the electron probability of being in the Ag orbital is reduced and smaller than that in the Cu orbital owing to the covalent character of the bonding with four nitrogens in the Ag–oep complex, as reported by the ESR studies of the Ag–porphyrin and Cu–porphyrin complexes [20]. In the Ag–oep complex, the modified point-dipole model using a reduced electron probability of 74% on the Ag  $4d_{x^2-y^2}$  orbital gives the  $r$  value of  $4.475 \text{ \AA}$ .

### 3.3. $\text{Ag}^{\text{II}}(\text{oep})\text{C}_{70}$

In this subsection, we comment on the ESR results of  $\text{Ag}^{\text{II}}(\text{oep})\text{C}_{70}$  polycrystalline samples, where the triplet spin states due to magnetic dipolar interactions is observed, as similar to  $\text{Ag}^{\text{II}}(\text{oep})\text{C}_{60}$ .

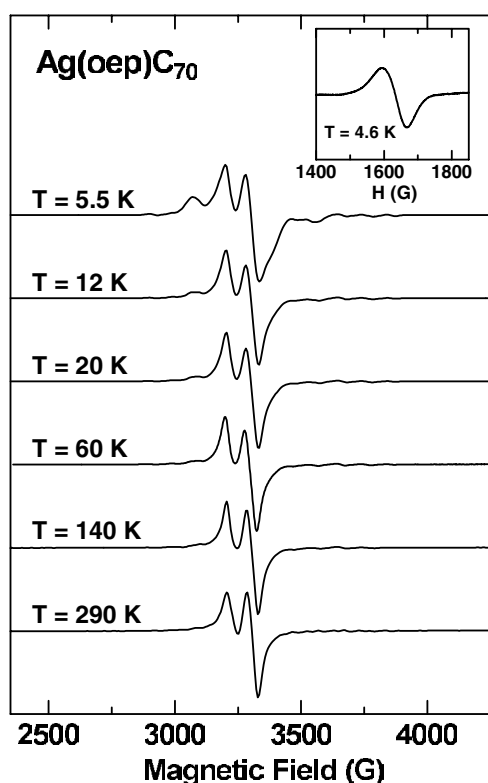


**Figure 6.** Temperature dependence of the ESR spectrum of  $\text{Ag}^{\text{II}}(\text{oep})\text{C}_{70}$  polycrystalline samples. Inset: ESR spectrum of  $\text{Ag}^{\text{II}}(\text{oep})\text{C}_{70}$  polycrystalline samples at half field of  $\sim 1600$  G.

Figure 6 shows the temperature dependence of the ESR spectrum of  $\text{Ag}^{\text{II}}(\text{oep})\text{C}_{70}$  polycrystalline samples. The inset of figure 6 shows the ESR spectrum at half field. The line shapes of these spectra are nearly independent of the temperature. The structure in the ESR spectra is ascribed to the fine structure of the triplet spin state due to magnetic dipolar coupling of  $\text{Ag}^{\text{II}}$  ions in the adjacent oep molecules, as discussed in  $\text{Ag}^{\text{II}}(\text{oep})\text{C}_{60}$ . The triplet spin state is also confirmed by the forbidden transition at half field (see the inset of figure 6). The  $\chi_s$  of  $\text{Ag}^{\text{II}}(\text{oep})\text{C}_{70}$  polycrystalline samples almost obeys the Curie law; the Curie-spin concentration is obtained as  $\approx 100\%$ . These results are similar to those of  $\text{Ag}^{\text{II}}(\text{oep})\text{C}_{60}$ , except for the splitting width of the fine structure.

Here, we compare the dipolar fine-structure splitting width between  $\text{Ag}^{\text{II}}(\text{oep})\text{C}_{60}$  and  $\text{Ag}^{\text{II}}(\text{oep})\text{C}_{70}$ . The  $D$  value estimated by the ESR intensity ratio of  $\chi_s^{g^4}/\chi_s$  is of the order of  $10^{-3} \text{ cm}^{-1}$  in  $\text{Ag}^{\text{II}}(\text{oep})\text{C}_{70}$ , which is smaller than that in  $\text{Ag}^{\text{II}}(\text{oep})\text{C}_{60}$ . This result is consistent with the smaller splitting width in the ESR spectra of  $\text{Ag}^{\text{II}}(\text{oep})\text{C}_{70}$  than that of  $\text{Ag}^{\text{II}}(\text{oep})\text{C}_{60}$  (see figures 3(a) and 6). Hence, the d-d distance in  $\text{Ag}^{\text{II}}(\text{oep})\text{C}_{70}$  seems to be larger than that in  $\text{Ag}^{\text{II}}(\text{oep})\text{C}_{60}$ . However, the recent x-ray studies show that the molecular packing in  $\text{Ag}^{\text{II}}(\text{oep})\text{C}_{70}$  is different from that in  $\text{Ag}^{\text{II}}(\text{oep})\text{C}_{60}$  and the d-d distance in  $\text{Ag}^{\text{II}}(\text{oep})\text{C}_{70}$  is smaller than that in  $\text{Ag}^{\text{II}}(\text{oep})\text{C}_{60}$  [18]. Thus, the results of the ESR studies apparently contradict those of the x-ray studies. Although this discrepancy is an interesting problem and the further ESR study using a single-crystalline sample is needed to solve this problem, the single-crystal ESR study has not been performed because single crystals with good quality have not been obtained so far, which is open for the future studies.

#### 4. Summary

We have investigated the newly synthesized  $\pi$ -d-electron system  $\text{Ag}^{\text{II}}(\text{oep})\text{C}_{60}$  and  $\text{Ag}^{\text{II}}(\text{oep})\text{C}_{70}$  by the ESR method using single-crystalline and polycrystalline samples. The fine-structure splitting due to the triplet-spin states is found in  $\text{Ag}^{\text{II}}(\text{oep})\text{C}_{60}$  and  $\text{Ag}^{\text{II}}(\text{oep})\text{C}_{70}$  owing to magnetic dipole-dipole interactions between adjacent  $\text{Ag}^{\text{II}}$  ions in the oep molecules. The single-crystal studies of  $\text{Ag}^{\text{II}}(\text{oep})\text{C}_{60}$  determine the angle between the direction of the fine-structure interaction and the normal of the porphyrin plane as  $37^\circ$ . The spin susceptibility of all complexes almost shows the Curie-law behaviour in the temperature region between 4 and 300 K. This feature is in contrast to the study of  $\text{Co}^{\text{II}}(\text{tbp})\text{C}_{60}$  that shows antiferromagnetic super-exchange interactions between  $\text{Co}^{\text{II}}$  spins via the  $\text{C}_{60}$  molecule. The absence of the super-exchange interaction is understood by the symmetry of the orbital wavefunction of metal ions; that is, the wavefunction extends to the oep plane, not to the  $\text{C}_{60}$  molecule in the present complexes. Thus, these ESR studies have successfully obtained the useful knowledge of the magnetic interactions such as magnetic dipolar and exchange interactions in the above  $\pi$ -d-electron system.

#### References

- [1] Kroto H W, Heath J R, O'Brien S C, Curl R F and Smalley R E 1985 *Nature* **318** 162
- [2] Hebard A F, Rosseinski M J, Haddon R C, Murphy D W, Glarum S H, Palstra T T M, Ramirez A P and Kortan A R 1991 *Nature* **350** 600
- [3] Allemand P M, Khemani K C, Koch A, Wudl F, Holczer K, Donovan S, Gruner G and Thompson J D 1991 *Science* **253** 301
- [4] Dyachenko O A and Graja A 1999 *Fullerene Sci. Technol.* **7** 317
- [5] Hardie M J and Raston C L 1999 *Chem. Commun.* 1153
- [6] Olmstead M M, Costa D A, Maitra K, Noll B C, Phillips S L, Van Calcar P M and Balch A L 1999 *J. Am. Chem. Soc.* **121** 7090
- [7] Boyd P D W, Hodgson M C, Rickard C E F, Oliver A G, Chaker L, Brothers P J, Bolskar R D, Tham F S and Reed C A 1999 *J. Am. Chem. Soc.* **121** 10487
- [8] Hochmuth D H, Michel S L J, White A J P, Williams D J, Ballet A G M and Hoffman B M 2000 *Eur. J. Inorg. Chem.* **2000** 593
- [9] Ishii T, Aizawa N, Yamashita M, Matsuzaka H, Kodama T, Kikuchi K, Ikemoto I and Iwasa Y 2000 *J. Chem. Soc. Dalton Trans.* **23** 4407
- [10] Ishii T, Aizawa N, Kanehama R, Yamashita M, Matsuzaka H, Kodama T, Kikuchi K and Ikemoto I 2001 *Inorg. Chim. Acta* **317** 81
- [11] Ishii T, Kanehama R, Aizawa N, Yamashita M, Matsuzaka H, Sugiura K, Miyasaka H, Kodama T, Kikuchi K, Ikemoto I, Tanaka H, Marumoto K and Kuroda S 2001 *J. Chem. Soc. Dalton Trans.* **20** 2975
- [12] Ishii T, Kanehama R, Aizawa N, Yamashita M, Matsuzaka H, Sugiura K and Miyasaka H 2002 *Coord. Chem. Rev.* **226** 113
- [13] Tanaka H, Marumoto K, Kuroda S, Ishii T, Kanehama R, Aizawa N, Matsuzaka H, Sugiura K, Miyasaka H, Kodama T, Kikuchi K, Ikemoto I and Yamashita M 2002 *J. Phys.: Condens. Matter* **14** 3993
- [14] Sun D, Tham F S, Reed C A, Chaker L and Boyd P D W 2002 *J. Am. Chem. Soc.* **124** 6604
- [15] Kahn O 1993 *Molecular Magnetism* (New York: VCH)
- [16] Marumoto K, Takeuchi N and Kuroda S 2003 *Chem. Phys. Lett.* **382** 541
- [17] Marumoto K, Muramatsu Y and Kuroda S 2003 *Appl. Phys. Lett.* **84** 1317
- [18] Ishii T, Kanehama R, Aizawa N, Yamashita M, Sugiura K, Miyasaka H, Kodama T, Kikuchi K and Ikemoto I 2004 *Intelligence in a Materials World: Nanotechnology for the 21st Century* part II, ed J A Meech, Y Kawazoe, V Kumar and J F Maguire (Lancaster, PA: DEStech Publications Inc.) chapter 11
- [19] Balch A L and Olmstead M M 1998 *Chem. Rev.* **98** 2123
- [20] Kneubühl F K, Koski W S and Caughey W S 1961 *J. Am. Chem. Soc.* **83** 1607
- [21] Orton J W 1968 *Electron Paramagnetic Resonance* (London: Iliffe)
- [22] Marumoto K, Tanaka H, Kozaki S, Kuroda S, Miya S, Kawashima T and Yamashita M 2001 *Solid State Commun.* **120** 101